

# Design and optimization of weakly-coupled few-mode fiber with low nonlinearity

Junyan Liu (刘俊彦)\*, Jie Zhang (张杰), Jiawei Han (韩佳巍), Guanjun Gao (高冠军),  
Yongli Zhao (赵永利), and Wanyi Gu (顾婉仪)

State Key Laboratory of Information Photonics and Optical Communications,  
Beijing University of Posts and Telecommunications, Beijing 100876, China

\*Corresponding author: liujunyan525@gmail.com

Received September 23, 2013; accepted January 15, 2014; posted online February 28, 2014

By investigating the influence of the difference of refractive index between core and cladding ( $n_{co} - n_{cl}$ ), normalized frequency ( $V$ ) and core radius ( $\alpha$ ) on both the intramodal and intermodal nonlinear coefficients (NCs) respectively, we design a novel weakly-coupled four-mode fiber with low nonlinearity. In general, under the premise of ensuring the low NCs between two non-degenerate modes, this design can reduce the intermodal NCs ( $< 0.5 \text{ W}^{-1} \cdot \text{km}^{-1}$ ) between two degenerate modes and optimizes the parameters of differential group delays (DGDs) and chromatic dispersion. The optimized few mode fiber (FMF) is eligible for transmission and mode de-multiplexing in the receiver.

OCIS codes: 060.2280, 060.4230, 190.3270.

doi: 10.3788/COL201412.030601.

Mode-division multiplexing (MDM) transmission in few mode fiber (FMF) has been regarded as a very promising choice for solving the “capacity crunch”<sup>[1]</sup> resulted from the rapid growth in data services. However, MDM has many urgent questions need to resolve, such as mode multiplexing and de-multiplexing, nonlinear effects, and mode coupling.

The requirements for FMF are similar to single-mode fiber (SMF): low attenuation, low loss, low nonlinearity (i.e., high effective area), and high dispersion coefficient<sup>[2]</sup>. However, there are also some special needs for designing a weakly-coupled FMF compared to SMF. Firstly, for the weakly-coupled FMF used for uncoupled MDM transmissions, large differential group delays (DGDs) are needed to use the multiple input, multiple output (MIMO) digital signal processing (DSP) with low complexity at the receiver side<sup>[3,4]</sup>. Moreover, a large difference of effective refractive index between any two modes help ensure the low mode coupling. The new design tradeoffs and MIMO DSP technology<sup>[5]</sup> have to be considered to process mode coupling, but actually the mode mixing arising from the Kerr nonlinear effects<sup>[6]</sup>. So it is worthy to design a FMF with low nonlinearity on the structure and large DGD.

Previous reported methods and techniques for designing FMF<sup>[7-11]</sup> give us a good possibility to investigate the performances of FMF. However, most of these studies on nonlinear related work only involves the definition

and simple calculations. In this letter, we investigate the relationship between nonlinearity coefficients (NCs) and many parameters respectively, and propose a method for designing weakly-coupled FMF with low nonlinearity (low intermodal NCs). Based on these investigations, we design a four-mode fiber with optimized DGD and other parameters, which is suitable for weakly-coupled few mode multiplexed systems.

The degenerate and non-degenerate linear modes are approximate solution at the state of weak wave guide in step-index fiber, and the number of the propagation mode is completely decided by the normalized frequency,  $V = 2\pi\alpha/\lambda\sqrt{n_{co}^2 - n_{cl}^2}$ , where  $n_{co}$  and  $n_{cl}$  are the refractive indexes of the core and the cladding,  $\alpha$  is the core radius, and  $\lambda$  is the wavelength respectively.

We choose  $V = 5.1$  for 4-mode transmission resulted from the mode power distribution. The 4 guided-mode in FMF could provide 6 spatial modes (include two pairs degenerate linear modes) and 2 polarization directions for MDM transmission. So it could offer an increasing transmission capacity with 6 times compared with the standard step-index single-mode fiber (S-SMF).

On the one hand, high ( $n_{eff,lm} - n_{cl}$ ) could ensure low macro-bend losses for the 4  $LP_{lm}$  modes, and large  $|n_{eff,lm} - n_{eff,l'm'}|$  between any two  $LP_{lm}$  and  $LP_{l'm'}$  modes is used to limit mode coupling<sup>[9]</sup>. On the other hand, small intramodal nonlinear effects and low losses could be ensured by large  $A_{eff}$ .

Table 1. Simulation of 4-mode FMF

$V=5.1, \lambda = 1.55 \mu\text{m}$	$LP_{01}$	$LP_{11a}(LP_{11b})$	$LP_{21a}(LP_{21b})$	$LP_{02}$
$n_{eff} - n_{cl} (\times 10^{-3})$	6.094	4.431	2.324	1.709
DGD vs $LP_{01}$ (ps/m)	0	3.498	6.809	4.761
Chromatic Dispersion ( $\text{ps}\cdot\text{nm}^{-1}\text{km}^{-1}$ )	10.94	12.38	10.00	0.11
Cable Cutoff Wavelength (nm)	/	2648	1836	1820
Macro-Bend Loss (10-mm bend loss) (dB/m)	$< 0.001$	0.005	15.621	938.867
$A_{eff} (\mu\text{m}^2)$	160.1	152.7 (151.7)	171.4 (170.3)	162.2
$\gamma$ -intramodal ( $\text{W}^{-1}\text{km}^{-1}$ )	0.658	0.690 (0.695)	0.615 (0.619)	0.650

The parameter values of the step-index optical fiber were obtained by modeling this following properties: core radius  $\alpha = 8.5 \mu\text{m}$  and  $n_{\text{co}} - n_{\text{cl}} = 7.2 \times 10^{-3}$ . Tables 1 and 2 are the relevant parameters. Particularly, data in parentheses are corresponding to the modes of LP<sub>11b</sub> or LP<sub>21b</sub> in the parentheses above.

To ensure small intermodal nonlinear effects in the fiber, and also well-separated non-degenerate modes at the receiver side, the DGDs between any two LP<sub>lm</sub> and LP<sub>l'm'</sub> modes are required<sup>[3]</sup>:

$$\text{DGD} = \left( \frac{n_{\text{eff},lm} - n_{\text{eff},l'm'}}{c} \right) - \frac{\lambda}{c} \left( \frac{\partial n_{\text{eff},lm}}{\partial \lambda} - \frac{\partial n_{\text{eff},l'm'}}{\partial \lambda} \right) \gg 0.1 \text{ ps/m.} \quad (1)$$

And model used for bend loss formula is

$$2\alpha = \frac{\sqrt{\pi} k^2 \exp \left[ -\frac{2}{3} \left( \frac{\gamma^3}{\beta_g^2} \right) R \right]}{e_\nu \gamma^{3/2} \sqrt{R} K_{\nu-1}(\gamma\alpha) K_{\nu+1}(\gamma\alpha)}, \quad (2)$$

where  $\gamma = (\beta_g^2 - n_2^2 k^2)^{1/2}$ ,  $\kappa = (n_1^2 k^2 - \beta_g^2)^{1/2}$ ,  $R$  is the radius of curvature, and  $\beta_g$  is the propagation constant of the guided mode in the straight guide. The  $K$  terms are modified Bessel functions, and  $\nu$  is azimuthal mode number<sup>[12]</sup>.

The Kerr nonlinear effect between two modes is often associated with the overlap integral  $f_{pq}$ :

$$f_{pq} = \frac{\iint |F_P(x,y)|^2 |F_Q(x,y)|^2 dx dy}{\iint |F_P(x,y)|^2 dx dy \iint |F_Q(x,y)|^2 dx dy}, \quad (3)$$

where the modes functions  $F_P(x,y)$  and  $F_Q(x,y)$  give the electric field distribution of the two modes respectively. The electric field distribution of degenerate modes (LP<sub>m1a</sub> and LP<sub>m1b</sub>) here are expressed by  $\psi_{m1a}(\gamma, \theta) = \psi_{m1}(\gamma) \cos(\theta)$  and  $\psi_{m1b}(\gamma, \theta) = \psi_{m1}(\gamma) \sin(\theta)$  respectively. The NC between the two modes is defined as

$$\gamma_{pq} = \frac{n_2 w_0 f_{pq}}{c} \frac{n_2 w_0}{c A_{\text{eff},pq}}, \quad (4)$$

where  $n_2$  is the nonlinear refractive index of silicon, which is about  $2.6 \times 10^{-20} \text{ m}^2/\text{W}$ ;  $\omega_0$  is the angular frequency of the carrier light and  $c$  is the speed of light<sup>[7]</sup>.

Obviously, modes LP<sub>11a</sub> and LP<sub>11b</sub> have equal intermodal NC with LP<sub>01</sub> or LP<sub>02</sub> respectively, as well as modes LP<sub>21a</sub> and LP<sub>21b</sub>. We use the symbol LP<sub>m1a/b</sub> sign LP<sub>m1a</sub> or LP<sub>m1b</sub>. There is a clear confirmation for the intermodal effective area between two degenerate spatial modes which is 3 times larger than the intramodal effective area respectively<sup>[8]</sup>, namely:

$$A_{\text{eff},pq} = 3 \cdot A_{\text{eff},p} = 3 \cdot A_{\text{eff},q}. \quad (5)$$

Besides, as shown from Table 2,  $A_{\text{eff}}$  between LP<sub>11a</sub> and LP<sub>21a</sub> has a tiny difference with the one between

LP<sub>11b</sub> and LP<sub>21b</sub>. This is because the angle between LP<sub>11a</sub> and LP<sub>21a</sub> is different from the angle between LP<sub>11b</sub> and LP<sub>21b</sub>. Moreover, with a largest intermodal NC, the nonlinear crosstalk between LP<sub>01</sub> and LP<sub>02</sub> might be more serious, which due to their largest regions of overlapped mode field.

Under the premise of ensuring the low NCs between two non-degenerate modes, low intermodal NCs between two degenerate modes could better ensure low nonlinearity for the weakly-coupled FMF, which is also preferable for independent transmission with low crosstalk between two non-degenerate linear modes. So we simulate the two categories of Kerr NCs on many cases of only one variable changes, and the relationship between all of NCs and the carrier light wavelength are shown in Fig. 1. Obviously, the intramodal NCs are more sensitive to wavelength and it also quickly reduced.

For the four linear polarized (LP) modes, LP<sub>11</sub> has the biggest intramodal NCs, followed are LP<sub>01</sub>, LP<sub>02</sub>, and LP<sub>21</sub>. Here the  $\gamma$ -LP<sub>11a</sub> curve has a tiny drop below the  $\gamma$ -LP<sub>11b</sub>, and it is same to the LP<sub>21a</sub> and LP<sub>21b</sub>. Further, the intramodal NCs could close to 1 if the core radius ( $\alpha$ ) decrease, but the intermodal NCs near 0.5.

Through our calculations, we also prove that the chromatic dispersion will decrease even to a negative value for one mode as the decreasing of  $n_{\text{co}} - n_{\text{cl}}$ . Thus we could use this rule to design the dispersion compensation fiber.

From Fig. 2(a), for a fixed  $V$  and  $\alpha$ , all of NCs are unchanged (virtually, they have several of ten thousandth difference if  $n_{\text{co}} - n_{\text{cl}}$  has a big difference) within the valid

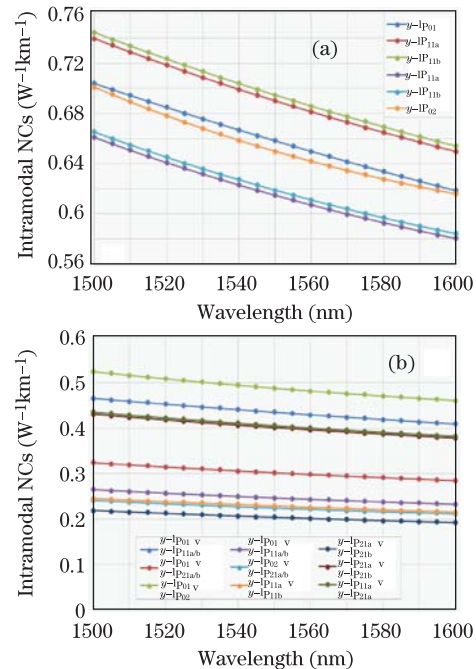


Fig. 1. (Color online) (a) Intramodal and (b) intermodal NCs as functions of wavelength respectively.

Table 2. Intermodal NCs of 4-Mode FMF

$A_{\text{eff}}$ and Nonlinear Effects of Intermodals	LP <sub>01v</sub>	LP <sub>01v</sub>	LP <sub>01v</sub>	LP <sub>02v</sub>	LP <sub>02v</sub>	LP <sub>11av</sub>	LP <sub>21av</sub>	LP <sub>11av</sub>	LP <sub>21av</sub>	LP <sub>11av</sub>	LP <sub>11bv</sub>
	LP <sub>11a/b</sub>	LP <sub>21a/b</sub>	LP <sub>02</sub>	LP <sub>11a/b</sub>	LP <sub>21a/b</sub>	LP <sub>11b</sub>	LP <sub>21b</sub>	LP <sub>21b</sub>	LP <sub>11b</sub>	LP <sub>21b</sub>	LP <sub>21b</sub>
$A_{\text{eff},pq} (\mu\text{m}^2)$	242.2	348.8	215.9	426.9	469.3	459.74	515.98	262.42	262.42	259.85	259.82
$\gamma$ -intermodal $(\text{W}^{-1}\text{km})^{-1}$	0.435	0.302	0.488	0.247	0.225	0.2292	0.2043	0.4016	0.4016	0.4056	0.4056

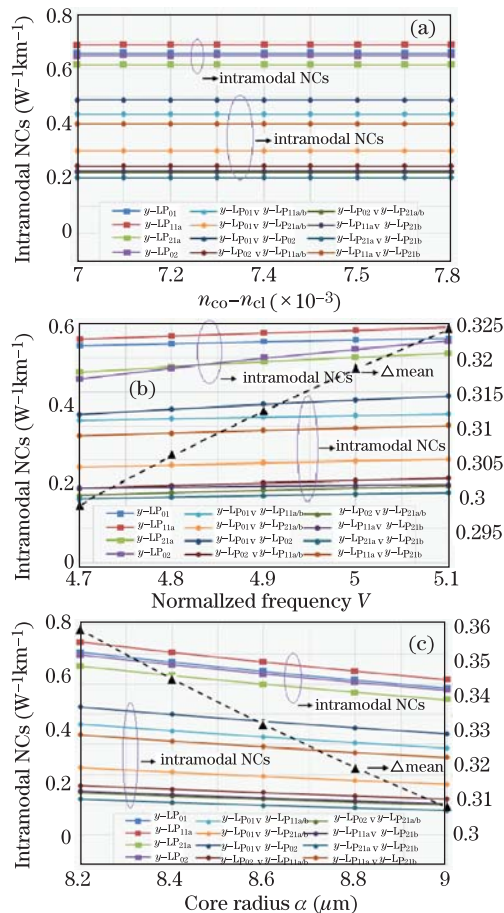


Fig. 2. (Color online) NCs as functions of (a)  $n_{co} - n_{cl}$  when  $V = 5.1$  and  $\alpha = 8.5 \mu\text{m}$ , (b) the normalized frequency ( $V$ ) when  $\alpha = 8.5 \mu\text{m}$ , and (c) core radius  $\alpha$  when  $V = 5.1$  at  $n_{co} - n_{cl} = 7.5 \times 10^{-3}$  and  $1550 \text{ nm}$  respectively.

range of  $n_{co} - n_{cl}$ . And a large value of  $n_{co} - n_{cl}$  at the state of weak wave guide is better to get a big numerical aperture.

Based on the above analysis, we choose  $n_{co} - n_{cl} = 7.5 \times 10^{-3}$  to study the relationship between NCs and normalized frequency  $V$  as show in Fig. 2(b), which has a apparent growth with  $V$  rising, and the intramodal NCs are growing faster than the intermodal, that can be reflected by the  $\Delta_{\text{mean}}$  line directly ( $\Delta_{\text{mean}}$  gives a difference between the mean of all the intra modal NCs and the mean of all the intermodal NCs). The result also could prove the mode power distribution theory indirectly (more mode power concentrate on the core when  $V$  growing large). Although larger mode power density in fiber core is disadvantage for low nonlinearity, it is beneficial for long-haul transmission due to the low loss. Figure 2(c) shows the trend of NCs within the different core radius ( $\alpha$ ), and it is a similar but decreasing trend along with the  $\alpha$  growing. Moreover, the intramodal NCs are more sensitive to  $\alpha$  than intermodal NCs, so a proper selection of  $\alpha$  is very necessary.

By using the above result of reducing fiber nonlinearity, we optimize this four-mode FMF to pursue weak coupling between any two modes. Through extensive simulations, a relative equilibrium difference between any two  $n_{\text{eff},lm}$  and low chromatic dispersions (shown in Table 1) are ob-

tained. The large DGDs between non-degenerate modes is required in uncoupled MDM link over weakly-coupled FMF, to enable the low-complexity  $2 \times 2$  or  $4 \times 4$  MIMO to be used at the receiver side.

In conclusion, we design a weakly-coupled FMF with low nonlinearity. Through simulating the two categories of Kerr nonlinear effects: intramodal and intermodal NCs, we draw some simple and useful conclusions: lower normalized frequency  $V$  for 4-mode FMF is suitable selection to get low nonlinearity, but a large one is necessary for long-haul transmission. NCs are unchanged within a rang value of  $n_{co} - n_{cl}$ , so a large value of  $n_{co} - n_{cl}$  at the state of weak guide is preferable. Big core radius ( $\alpha$ ) seems better if we have enough capacity of compensation in the receiver. Under the premise of ensuring the low NCs between two non-degenerate modes, we reduce the intermodal NCs ( $< 0.5 \text{ W}^{-1} \cdot \text{km}^{-1}$ ) between two degenerate modes, and optimize the parameters of DGDs and chromatic dispersion. Compared with the previous reported FMF, the performances of the 4-mode FMF we designed with lower mode coupling and lower NCs are more superior, and it is also more eligible for weakly coupled few-mode transmission.

This work was supported by the National “973” Program of China (Nos. 2010CB328204 and 2014CB340102), the National “863” Program of China (No. 2012AA011301), the National Natural Science Foundation of China (Nos. 61302085, 61271191, and 61271189), and the China Post-Doctoral Foundation Project (No. 2012M520207).

## References

1. R. W. Tkach, in *Proceedings of 36th European Conference and Exhibition on Optical Communication (ECOC)* We.7.D.1 (2010).
2. L. Grüner-Nielsen, Y. Sun, J. W. Nicholson, D. Jakobsen, K. G. Jespersen, R. Lingle, and B. Pálsdóttir, *J. Lightwave Technol.* **30**, 3693 (2012).
3. P. Sillard, M. Astruc, D. Boivin, H. Maerten, and L. Provost, in *Proceedings of European Conference and Exhibition on Optical Communication (ECOC)* Tu.5.LeCervin.7 (2011).
4. J. Han and J. Zhang, *Opt. Lett.* **37**, 3546 (2012).
5. B. Franz, D. Suikat, R. Dischler, F. Buchali, and H. Buelow, in *Proceedings of European Conference and Exhibition on Optical Communication (ECOC)* Tu.3.C.4 (2010).
6. F. Ferreira, S. Jansen, P. Monteiro, and H. Silva, *IEEE Photon. Technol. Lett.* **24**, 240 (2012).
7. C. Koebele, M. Salsi, G. Charlet, and S. Bigo, in *Proceedings of European Conference and Exhibition on Optical Communication (ECOC)* Mo.2.C.6 (2010).
8. C. Koebele, M. Salsi, G. Charlet, and S. Bigo, *IEEE Photon. Technol. Lett.* **23**, 1316 (2011).
9. R. Olshansky, *Appl. Opt.* **14**, 935 (1975).
10. D. Boivin, M. Bigot-Astruc, M. Travagnin, and P. Sillard, in *Proceedings of Optical Fiber Communication Conference OTh3K.6* (2013).
11. M. Bigot-Astruc and P. Sillard, in *Proceedings of Optical Fiber Communication Conference OTh4I.1* (2012).
12. D. Marcuse, *J. Opt. Soc. Am.* **66**, 216 (1976).